

Architectural Effect on the Surface Tension of an ABA Triblock Copolymer Melt

M. W. Matsen*

Department of Mathematics, University of Reading, Whiteknights, Reading RG6 6AX, U.K.

Received October 2, 2009; Revised Manuscript Received December 1, 2009

By carefully comparing ABA triblock copolymers with chemically matched AB diblock copolymers, Khanna et al.¹ have recently shown that molecular architecture affects the surface energy of an ordered block copolymer melt. In particular, their experiment revealed a greater tendency for the B-rich domains of the diblock copolymer melt to form at the surface than those of the triblock copolymer melt, a result that they confirmed with self-consistent field theory (SCFT).^{2,3} This behavior was attributed to the effect the surface has on the configurations of ABA triblock copolymers. Normally, the middle B blocks exhibit a mixture of bridging and looping configurations,⁴ but the opportunity for bridging is lost in domains adjacent to a surface. Khanna et al. suggested that the resulting loss in entropy was responsible for the elevated surface energy of the B-rich domains formed from ABA triblock copolymers. In fact, this entropic effect was proposed more than a decade ago by de Jeu et al.,⁵ but only now is there experimental evidence to support it.

Although this explanation for the experiment sounds sensible, we must not forget that all polymer segments, including those of the end-blocks, experience a reduction in entropy in the presence of a surface. For the flexible Gaussian chains used in SCFT, the entropic contribution to the surface tension should be well approximated by²

$$\gamma \approx \frac{a^2 \rho_0 k_B T}{24} \int \frac{[\phi_0'(z)]^2}{\phi_0(z)} dz \quad (1)$$

where a is the statistical segment length and ρ_0 is the segment density. This expression is derived assuming that the total polymer concentration, $\phi_0(z) = \phi_A(z) + \phi_B(z)$, decreases sharply from its bulk value to zero at the surface, and it should apply equally to both end-block and mid-block domains.

To resolve this apparent contradiction, we reconsider the SCFT calculation of Khanna et al.¹ focusing on a surface in contact with the lamellae of an ABA triblock copolymer melt. Our calculation is done for a symmetric triblock composition of (0.25:0.5:0.25) at an intermediate segregation of $\chi N = 50$, where the domains are reasonably pure and composition fluctuations are relatively unimportant. (Here χ is the usual Flory–Huggins interaction parameter, and N is the total number of segments per triblock.) The narrow profile over which the polymer concentration drops to zero is, in principle,⁶ determined by balancing the enthalpic energy, which favors a steplike profile, and the entropic contribution, which favors a broad profile. However, we are not concerned with the type of surface (e.g., whether it be with air, an immiscible polymer, or a hard wall), nor are we interested in predicting the actual concentration profile; our aim is to understand how the entropy loss due to the surface is affected by the

block copolymer architecture. Therefore, as in ref 1, we impose the surface by simply constraining the overall polymer concentration, $\phi_0(z) \equiv \phi_A(z) + \phi_B(z)$, to a hyperbolic shape

$$\phi_0(z) = \frac{1}{2} \left[1 + \tanh\left(\frac{2z}{w_s}\right) \right] \quad (2)$$

where w_s controls the width of the surface. Unlike ref 1, however, we restrict our attention to chemically neutral surfaces so as to focus on the entropic effects.

For a given width, w_s , we solve the free energy, F , for parallel lamellae in an effective volume of $V = AL$ with a surface area of A and a reflecting boundary at $z = L$. The calculation follows ref 1, except that we solve the SCFT equations using a Fourier cosine expansion analogous to the sine expansion described in the Appendix of ref 7. The excess surface energy is then given by $\gamma = (F - F_b)/A$, where F_b is the bulk free energy for an equal volume of material. The value of L is chosen sufficiently large and adjusted such that γ is a local minimum, so that the lamella centered at $z = L$ corresponds to bulk conditions. Furthermore, we use a generous number of cosine terms in our expansion (up to 600) to ensure that the numerical inaccuracies are absolutely negligible. Figure 1a compares the resulting surface tension for the A- and B-rich domains, γ_A and γ_B , respectively, to the analytical result

$$\gamma \approx \frac{a^2 \rho_0 k_B T}{12 w_s} \quad (3)$$

obtained by evaluating eq 1 for the profile in eq 2. As expected, both γ_A and γ_B converge to the expression in eq 3 as the width of the surface, w_s , narrows.

Nevertheless, for finite widths, there is a residual difference in the tensions, $\Delta\gamma \equiv \gamma_B - \gamma_A$, which we plot in Figure 1b. Just as in the experiments and SCFT calculations of Khanna et al.,¹ the surface favors the A-rich domain formed from the end-blocks. However, it is now evident that $\Delta\gamma$ has a strong dependence on the width of the surface, w_s , from which it follows that the elevated value of γ_B cannot be attributed to the loss of bridging configurations. Bridges are either allowed or not allowed, and so if this was the underlying explanation, then $\Delta\gamma$ should not exhibit any significant w_s dependence. Furthermore, it is γ_A rather than γ_B that deviates most significantly from eq 3, indicating that the difference, $\Delta\gamma$, actually has something to do with the A-rich domains.

An important clue to the origins of $\Delta\gamma$ can be found by looking at the distribution of the individual segments.⁴ These are calculated from the partition function, $q(z,s)$, for the first sN segments of the chain ($0 \leq s \leq 1$) with the sN -th segment constrained at a

*E-mail: m.w.matsen@reading.ac.uk.

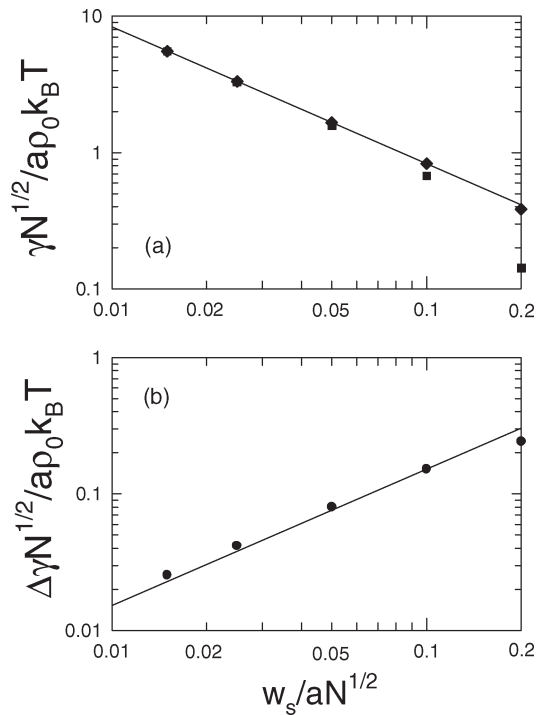


Figure 1. (a) Surface tensions, γ_A and γ_B , of the A-rich (square symbols) and B-rich (diamond symbols) domains, respectively, of an ABA triblock copolymer lamellar morphology as a function of the width of the surface, w_s . The line denotes the prediction in eq 3. (b) Difference in surface tensions, $\Delta\gamma \equiv \gamma_B - \gamma_A$ (circular symbols). The line shows the prediction in eq 6.

fixed distance, z , from the surface. It is obtained by solving a modified diffusion equation, starting from the initial condition, $q(z,0) = 1$. Once $q(z,s)$ is known, the distribution of the sN -th segment is immediately evaluated as $q(z,s)q(z,1-s)V|\mathcal{Q}$, where $\mathcal{Q} \equiv A \int q(z,1) dz$.

Figure 2a plots the distribution of the end segments, $\rho_e(z) = q(z,0)q(z,1)V|\mathcal{Q}$ (solid curve), within an A-rich domain, $\phi_A(z)$, next to the surface (dashed curve). For comparison purposes, we also show $\rho_e(z)$ from a layer in the bulk (dotted curve). Figure 2b is an analogous plot for the distribution of middle segments, $\rho_m(z) = q^2(z,1/2)V|\mathcal{Q}$, within a B-rich layer adjacent to the surface. While the profile of the middle segments is proportional to $\phi_0(z)$ at the surface, the end segments exhibit a broader profile proportional to $[\phi_0(z)]^{1/2}$. The reason for this is related to the ground-state dominance approximation^{2,8} used to derive eq 1. In the vicinity of a rapidly changing segment profile, the partition function takes the form $q(z,s) \approx c[\phi_0(z)]^{1/2} \exp(\lambda s)$ for sufficiently large s , where c and λ are constants. Apart from the few segments near the chain ends, most segments exhibit a distribution proportional to $\phi_0(z)$ at the surface. The chain ends, however, have a broader distribution because $q(z,s)$ remains relatively uniform for small s . The broader distribution, in turn, implies a greater amount of configurational entropy for the chain.

From this explanation, it follows that the chain-end effect can be removed by switching the initial condition from $q(z,0) = 1$ to $q(z,0) = [\phi_0(z)]^{1/2}$, which we have confirmed numerically. Since this is equivalent to applying a potential, $U_e(z) \equiv -k_B T \ln[\phi_0(z)]^{1/2}$, to the end segments, the extra entropic free energy associated with the broader chain-end distribution can be approximated as

$$\Delta\gamma \approx \frac{1}{A} \int \frac{\mathcal{D}F}{\mathcal{D}U_e} U_e dr = \frac{\rho_0}{N} \int \rho_e(z) U_e(z) dz \quad (4)$$

where the functional derivative is evaluated about $U_e(z) = 0$. With this linear approximation, the change in free energy due to

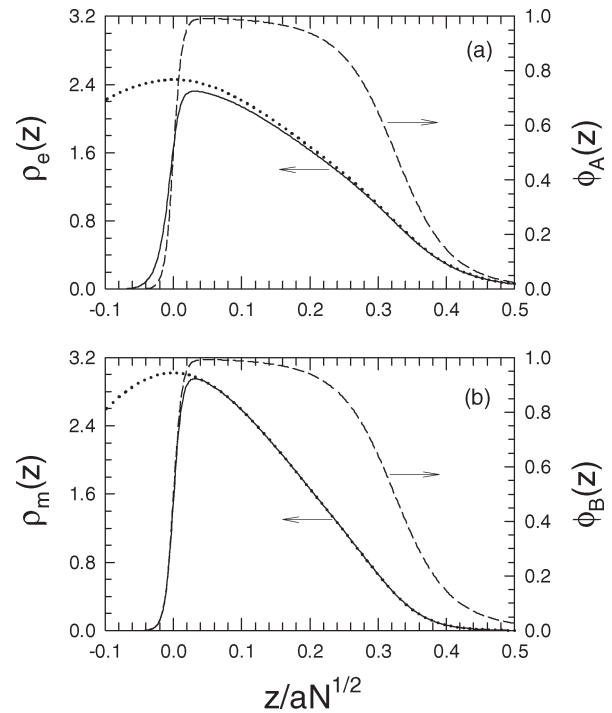


Figure 2. (a) Comparison of the end-segment distribution, $\rho_e(z)$, of an A-rich domain next to the surface (solid curve) of width $w_s = 0.025aN^{1/2}$ to that of an A-rich domain in the bulk (dotted curve). Also shown is the profile, $\phi_A(z)$, of an A-rich domain next to the surface (dashed curve). (b) Analogous plot for the middle-segment distribution, $\rho_m(z)$, of a B-rich domain.

$U_e(z)$ simply equates to the average internal energy due to $U_e(z)$. Because $U_e(z) \approx 0$ for $z \gtrsim w_s$, we can then approximate the end-segment distribution as $\rho_e(z) \approx \rho_e^* [\phi_0(z)]^{1/2}$, where $\rho_e^* = 2.46$ is the value of $\rho_e(z)$ in the middle of a bulk A-rich lamellae (see the dotted curve in Figure 2a). Thus, it follows that

$$\Delta\gamma \approx -\frac{\rho_e^* \rho_0 k_B T}{N} \int \sqrt{\phi_0(z)} \ln \sqrt{\phi_0(z)} dz \quad (5)$$

Evaluating this integral for the profile in eq 2 gives

$$\Delta\gamma \approx 0.617 w_s \rho_e^* \rho_0 k_B T / N \quad (6)$$

which is plotted in Figure 1b (solid line). The agreement with the SCFT calculation (circular symbols) is reasonably good over the given range of w_s . We note that Meng and Wang⁹ have also used end-segment entropy to explain their SCFT results showing a preference for diblock copolymer lamellae to orient parallel versus perpendicular to a surface, but they did not provide a calculation or derivation to confirm this hypothesis. However, a similar expression to eq 6 has been derived for the surface tension of a polymer melt.¹⁰

In addition to providing a corrected explanation for $\Delta\gamma$, our study also reveals a valuable simplification to the numerical treatment of the surface. Despite the connectivity of the polymer chains, the effects of a narrow surface remain localized to $z \lesssim w_s$. For example, the perturbations to the surface profiles (solid curves) relative to the bulk profiles (dotted curves) of $\rho_e(z)$ and $\rho_m(z)$ in Figure 2 vanish as w_s decreases. This allows us to dispense with the mask, $\phi_0(z) = \phi_A(z) + \phi_B(z)$, and instead solve the SCFT with the standard incompressibility condition, $\phi_A(z) + \phi_B(z) = 1$, combined with a reflecting boundary condition at $z = 0$, which is far less computationally demanding. When doing this, however, the

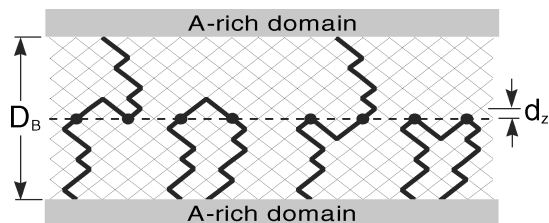


Figure 3. A group, i , of B-block configurations obtained by independently reflecting the three portions of the chain about the midplane (dashed line) defined by the $n_i = 2$ crossing points (solid dots). Note that the group contains the four additional configurations obtained by reflecting the left-most portion of each configuration shown above. Here the chains are restricted to a bcc lattice, such that each step of length a corresponds to a distance of $d_z = a/\sqrt{3}$ in the normal direction.

various surface effects must be inserted into the SCFT by hand. For instance, the end-segment effect responsible for $\Delta\gamma$ can be treated by a delta-function potential at $z = 0$ acting on the end segments, which in turn can be adsorbed into the initial condition for $q(z,s)$. The main entropic contribution to the surface tension, γ , in eq 1 is irrelevant for conformationally symmetric molecules (i.e., $a_A = a_B \equiv a$), since it just adds a constant to the free energy. However, for conformationally asymmetric molecules, it introduces a surface affinity for the component with the smaller segment length consistent with experiment¹¹ and previous SCFT calculations.¹² This entropic surface affinity can then be incorporated with the enthalpic surface affinity as a delta-function potential at the surface, which in turn can be adsorbed into the boundary condition.¹³ There is also a positive line tension that occurs when an A/B interface intercepts the surface,^{7,9} but this too can be treated by an appropriate surface interaction.

Although we have demonstrated that the entropy of bridging and looping does not effect the SCFT calculation of $\Delta\gamma$, the result is not particularly illuminating. For a more intuitive understanding, we reevaluate the entropy loss of creating an interface through the middle of a B domain of volume $V = AD_B$ with n chains, this time using a simple lattice-based treatment. In our lattice model, the N_B monomers of a B block are restricted to the sites of a bcc lattice, with the bonded monomers separated by one lattice constant, a . In general, a configuration will have n_i monomers on the midplane dividing the chain into $n_i + 1$ portions, as illustrated in Figure 3 for $n_i = 2$. From it, we can generate a group, i , of $g_i = 2^{n_i+1}$ configurations by independently reflecting each portion of the chain about the midplane. As note by Silberberg,¹⁴ each member of this group will occur with the same probability, P_i , assuming that the chain is completely flexible. Thus, the entropy of n B blocks can be expressed as

$$S_B = -nk_B \sum_i g_i P_i \ln P_i \quad (7)$$

where the probabilities are chosen so as to fill space uniformly with

$$\sum_i g_i P_i = 1 \quad (8)$$

Now if we disallow bridging, half of the configurations in each group are lost (i.e., $g'_i = g_i/2$), apart from those groups with $n_i = 0$. To continue to fill space, we must then increase the probabilities, P_i , appropriately. As it happens, the concentration distribution of the disallowed configurations exactly matches that of the allowed configurations. Thus, the uniform concentration is maintained by simply doubling the probabilities (i.e., $P'_i = 2P_i$)

for those groups with $n_i \geq 1$ and leaving the probabilities unchanged (i.e., $P'_i = P_i$) for groups with $n_i = 0$. It follows that the removal of bridges reduces the entropy by

$$\Delta S = -nk_B \sum_i g'_i P'_i \ln P'_i - S \quad (9)$$

$$= -nk_B (1 - \langle \delta_{0,n_i} \rangle) \ln 2 \quad (10)$$

where $\langle \delta_{0,n_i} \rangle$ is the average number of B blocks that never reach the midplane. Note that $\langle \delta_{0,n_i} \rangle = 1 - 2\nu_B$, where $\nu_B \approx 0.4$ is the equilibrium bridging fraction in a B lamellae.¹⁵ Of course, introducing a surface along the midplane not only disallows bridges, but also all configurations that otherwise would cross the midplane. In this case, each group is reduced to exactly two configurations (i.e., $g'_i = 2$), one on each side of the midplane. Again uniform concentration can be maintained by simply scaling up the probability of the remaining configurations by $P'_i = 2^{n_i} P_i$. Inserting this into eq 9, the change of entropy from preventing chains crossing the midplane is

$$\Delta S = -nk_B \langle n_i \rangle \ln 2 \quad (11)$$

where $\langle n_i \rangle$ is the average number of monomers a B block has at the midplane. Assuming that the B domain is pure, it follows that

$$\langle n_i \rangle = \frac{d_z N_B}{D_B} = \frac{aN_B}{\sqrt{3}D_B} \quad (12)$$

For normal situations where the contour length of a B block is much longer than the domain width (i.e., $aN_B \gg D_B$), $\langle n_i \rangle \gg 1$ and thus the entropy loss from preventing chains crossing the midplane (eq 11) dwarfs that due to disallowing bridges (eq 10). In any case, it immediately follows from eqs 11 and 12 that

$$\gamma = \frac{-T\Delta S}{2A} = a\rho_0 k_B T \frac{\ln 2}{2\sqrt{3}} \quad (13)$$

where we have used $n = AD_B\rho_0/N_B$ and the fact that splitting the B domain down the middle produces two surfaces of area A . Notice that this result is consistent with eq 3, since $w_s \approx a$ for our lattice calculation.

There is nothing in the derivation of eq 13 that is specific to the B blocks, and thus it applies equally to an A domain, where each chain is only attached to one of the two interfaces. Thus, $\Delta\gamma$ completely vanishes, which is because the lattice treatment assumed a step profile. The SCFT also predicts $\Delta\gamma \rightarrow 0$ as $w_s \rightarrow 0$, but in this case $\gamma \rightarrow \infty$. Unlike the freely jointed chains in the lattice model, Gaussian chains have a zero Kuhn length and an infinite contour length, although in such a way that the natural end-to-end length, $aN^{1/2}$, remains finite.¹⁶ Consequently, if a Gaussian chain crosses the midplane, it does so an infinite number of times. Indeed, if we take the Gaussian-chain limit, by increasing N_B at fixed $D_B/aN_B^{1/2}$, then $\langle n_i \rangle$ in eq 12 diverges. Hence, the lattice calculation is perfectly consistent with the SCFT results.

In summary, our SCFT calculation reconfirms the entropic preference of placing end-block domains next to a surface in comparison to mid-block domains, as previously demonstrated in ref 1. However, we find that the effect vanishes as the surface profile, $\phi_0(z)$, becomes sharper, which contradicts the explanation that mid-block domains avoid the surface because this prohibits bridging configurations. We show that the difference in surface tensions, $\Delta\gamma$, is actually related to the presence of chain ends at the surface. This is because end segments exhibit a broader distribution near a surface than middle segments, and thus they lose less entropy in the presence of a surface. With this corrected interpretation of the architectural effect on the surface energy of a

block copolymer melt, we should be able to reliably anticipate its extension to other block copolymer architectures, such as A_2B stars where the A- and B-rich domains will have different end-segment populations.

Acknowledgment. We are grateful to Glenn Fredrickson, Ian Hamley, Ed Kramer, and Dave Morse for useful discussions. This work was supported by the EPSRC (EP/G026203/1).

References and Notes

- (1) Khanna, V.; Cochran, E. W.; Hexemer, A.; Stein, G. E.; Fredrickson, G. H.; Kramer, E. J.; Li, X.; Wang, J.; Hahn, S. F. *Macromolecules* **2006**, *39*, 9346.
- (2) Matsen, M. W. In *Soft Matter*; Gompper, G., Schick, M., Eds.; Wiley-VCH: Weinheim, Germany, 2006; Vol. 1, Chapter 2.
- (3) Fredrickson, G. H. *The Equilibrium Theory of Inhomogeneous Polymers*; Oxford University Press: New York, 2006.
- (4) Matsen, M. W.; Thompson, R. B. *J. Chem. Phys.* **1999**, *111*, 7139.
- (5) de Jeu, W. H.; Lambooy, P.; Hamley, I. W.; Vaknin, D.; Pederson, J. S.; Kjaer, K.; Seyger, R.; van Hutten, P.; Hadziioannou, G. *J. Phys. II* **1993**, *3*, 139.
- (6) Actual surface profiles may be too sharp for a coarse-grained approach such as SCFT to be accurate, but it should still provide qualitatively correct trends.
- (7) Matsen, M. W. *J. Chem. Phys.* **1997**, *106*, 7781; note that a factor of V_0/V is missing from inside the logarithms of eqs 7 and A20.
- (8) de Gennes, P.-G. *Scaling Concepts in Polymer Physics*; Cornell University Press: Ithaca, NY, 1979.
- (9) Meng, D.; Wang, Q. *J. Chem. Phys.* **2007**, *126*, 234902.
- (10) Wu, D. T.; Fredrickson, G. H.; Carton, J.-P.; Ajdari, A.; Leibler, L. *J. Polym. Sci., Part B* **1995**, *33*, 2373.
- (11) Sikka, M.; Singh, N.; Karim, A.; Bates, F. S. *Phys. Rev. Lett.* **1993**, *70*, 307.
- (12) Wu, D. T.; Fredrickson, G. H. *J. Chem. Phys.* **1996**, *104*, 6387.
- (13) Matsen, M. W.; Griffiths, G. H. *Eur. Phys. J. E* **2009**, *29*, 107.
- (14) Silberberg, A. *J. Colloid Interface Sci.* **1982**, *90*, 86.
- (15) Matsen, M. W.; Schick, M. *Macromolecules* **1994**, *27*, 187.
- (16) Morse, D. C.; Fredrickson, G. H. *Phys. Rev. Lett.* **1994**, *73*, 3235. Matsen, M. W. *J. Chem. Phys.* **1996**, *104*, 7758.